ACS APPLIED ENERGY MATERIALS

www.acsaem.org

Forum Article

Bioderived Radical Polymers for Sustainable Energy Storage Materials

Scott L. Brooks, Zihao Liang, Hyunki Yeo, Bryan W. Boudouris,* and Andrew C. Weems*

Cite This: https://doi.org/10.1021/acsaem.3c02060

Read Online

ACCESS | Metrics & More | Article Recommendations | Supporting Information

ABSTRACT: Organic mixed ionic and electronic conductors have emerged as promising materials for next-generation energy applications, and a variety of molecular designs have been implemented to push performance to higher levels. Importantly, nonconjugated redox-active radical polymers capable of charge transport offer benefits such as ready synthesis in large quantities and the capability to separate thermomechanical and electrochemical behaviors. This affords more freedom with respect to macromolecular backbone design; thus, the resultant materials properties make this class of polymers appealing alternatives for energy storage. However, these radical polymers often still rely on petrochemically derived polymer backbones. Here, we demonstrate the polymerization of the bioderived terpene β-myrcene and its functionalization by attaching stable radical pendant groups capable of mixed electronic and ionic conduction. The electrochemical enhancement of these materials was substantial as the addition of carbon black and doping of lithium salts electronic conductivities of ~60 S cm^{-1} were achieved for the composite systems. The addition of the lithium salts proved fruitful as the electric and ionic conductivities of the radical polymers surpassed 10^{-4} S cm^{-1} at elevated temperatures when both lithium hexafluorophosphate and lithium chloride, a more bio and environmentally friendly material, where introduced to the system. These findings demonstrate a bioderived alternative for an organic mixed conductor serving as both potential cathode and polymer electrolyte for a more sustainable alternative for energy storage applications.

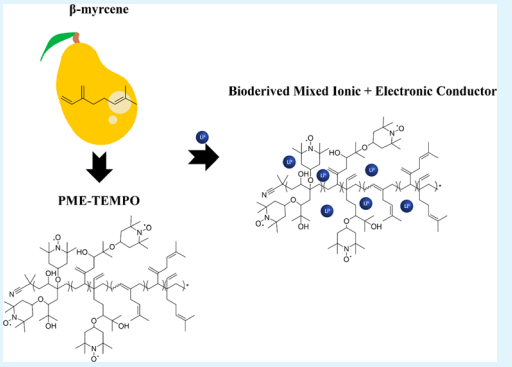

KEYWORDS: *Bioderived materials, Polymers for energy storage, Organic batteries, Organic mixed ionic-electronic conductors, Terpene derivatives*

INTRODUCTION

Electronically active polymers have garnered recent interest due to their potential to supplement or replace their inorganic counterparts in targeted applications.[1−3] To date, the majority of these materials are π-conjugated polymers; however, the syntheses of these advanced conducting materials often includes the use of metal-based catalysts that prove difficult to remove from the final polymer product, which leads to potential toxicity and environmental risks.[4−10] This is in tandem with potential for these materials to cause unintentional doping of the organic material that leads to degradation of long-term performance.[11,12] Of particular interest are oxidation−reduction-active (redox-active), radical-laden polymers composed of aliphatic backbones with pendant stable radical groups. These redox-active radical polymers are an appealing alternative and play a vital role in a variety of organic electronic applications.[13−16] These redox-active polymers offer several advantages, such as the ability to create homo- and copolymers through various synthetic mechanisms as well as create materials where the thermomechanical and electrochemical properties are not intertwined.[17] These synthetic methods create simpler routes of producing materials with complex architectures at scale for energy storage.[17−21] Additionally, through the selective addition and functionalization of pendant groups, preferentially oxidized radical polymers are useful cathode materials.[8,18,19,22] Thus, nonconjugated macromolecules offer the molecular architecture and thermomechanical properties desired for a variety of energy storage materials.

At the center of the redox functionality of these polymers are the stable radical groups.[23] A common open-shell group is the (2,2,6,6-tetramethyl-piperidin-1-yl)oxidanyl (TEMPO) pendant moiety, which is a frequently used electronically active site in nonconjugated materials.[7,24] Moreover, these pendant radical groups can undergo rapid charge transfer reactions with a high degree of stability and withstand the harsh conditions that can be associated with device performance.[25,26]

Special Issue: Organic Battery Materials

Received: August 17, 2023
Revised: November 1, 2023
Accepted: November 2, 2023

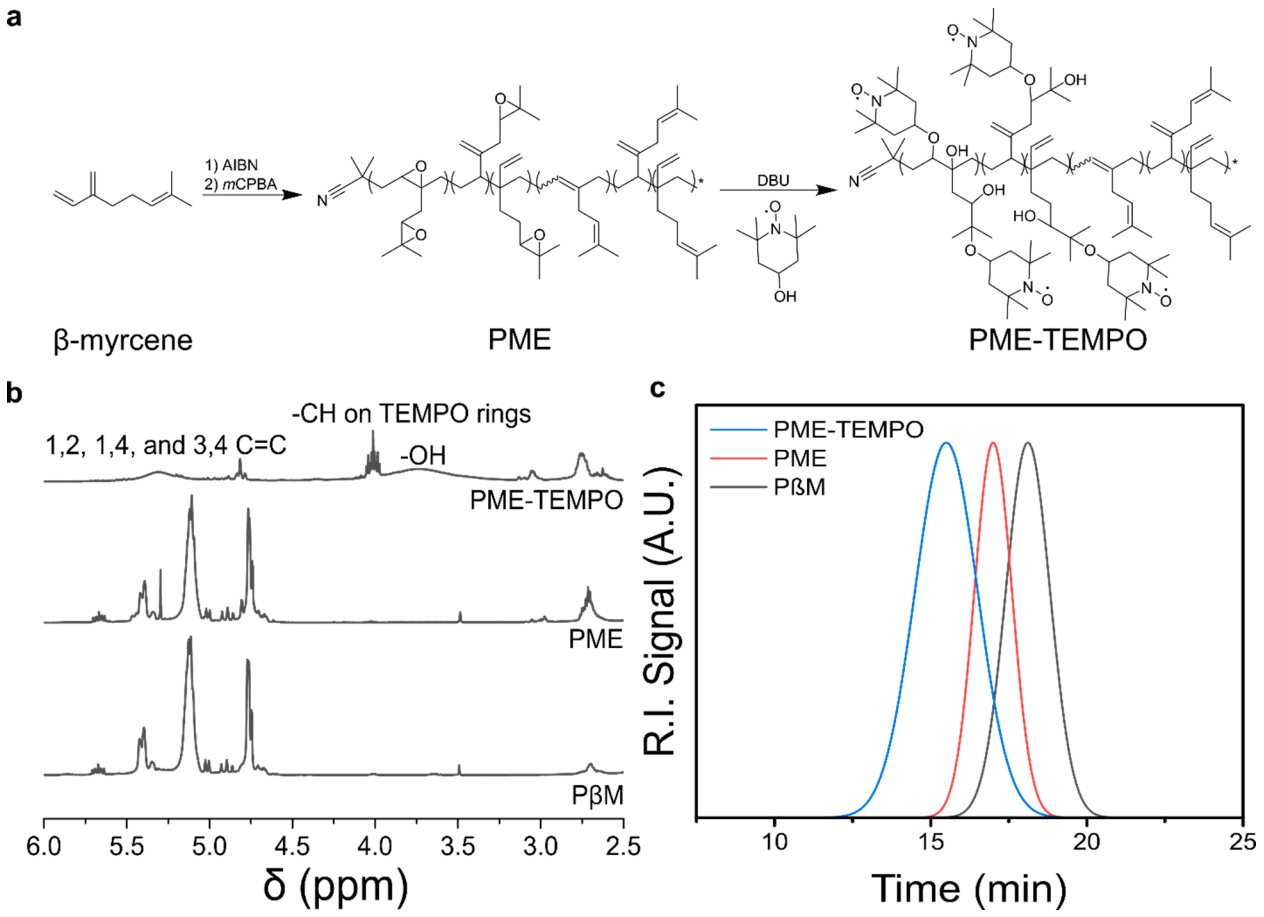

Figure 1. (a) Synthetic scheme showing the progression from the monomer, β-myrcene, to poly(myrcene-epoxide) (PME) via epoxidation, and the ring opening addition of hydroxy-TEMPO (H-TEMPO) using the organobase catalyst DBU to create the PME-H-TEMPO species (PME-TEMPO) via free radical polymerization (FR). (b) Representative ^{1}H NMR spectra of PβM, PME, and PME-TEMPO. (c) Representative SEC chromatograms showing that the hydrodynamic diameter of the material increases at each synthetic progression.

Another crucial factor to the performance of radical polymers is the charge density of the stable radical sites capable of undergoing reversible redox reactions along the polymer chain, as this can strongly impact the ability for these radical polymers to transport charge.[27−29] The nitroxide functionality within TEMPO is capable of readily undergoing redox reactions and allowing for electron exchange reactions between neighboring pendant groups, making it highly effective in energy storage applications.[30−32]

TEMPO is a commonly utilized radical bearing moiety in organic energy storage systems. The Suga and Nishide groups demonstrated radical content of nearly 100% for a series of different polymers, including poly(2,2,6,6-tetramethylpiperidinyloxy-4-yl methacrylate) (PTMA), poly(TEMPO-substituted norbornene), and a five-membered cyclic nitroxide material attached to a poly(ethylene oxide) backbone.[10,22,33] Multiple TEMPO-containing cyclic ethers have shown redox potentials of +3.66 V with a carbon composite cathode relative to a lithium anode.[34] Moreover, the use of a glycidyl-TEMPO material achieved an electrical conductivity of 0.28 S cm^{-1}.[7,8,23] This high conductivity can be achieved across significant molecular distances when the radical functional groups are arranged in periodical orders to facilitate charge transport.[35,36] Additionally, the Lutkenhaus group demonstrated biTEMPO-functionalized polypeptides for p-type cathodes in organic radical batteries, where the battery achieved could undergo more than 200 charge/discharge cycles without significant performance drop.[37] These examples highlight that organic open-shell radical polymers have proved to be a step in the right direction toward sustainable materials for energy storage.

Despite the success that radical polymers have had in emerging applications, the majority of these TEMPO-containing polymers are petrochemically derived.[38,39] Naturally derived materials, which contain a variety of functional moieties that may be leveraged for different applications, provide an alternative feedstock for polymers. One important class of functional natural products is terpenes, which are isolated from essential oils and often contain alkenes or other moieties useful in polymer synthesis.[40−44] Limonene, perhaps the best known terpene, is used in thermoplastic and thermoset polymer synthesis; however, often this consumes the majority of the useful alkenes.[45−47] Conversely, β-myrcene, a monoterpene that contains three alkene groups, can be polymerized into different stereochemistry linkages that result residual in-chain and side-chain alkenes.[48−50] This has made it of utility in multiple demonstrations. For example, Constant et al., produced poly(β-myrcene) and poly(limonene-*co*-β-myrcene) polymers suitable for vat photopolymerization 3D printing as an extension of previous work that had focused on homo poly(β-myrcene).[51,52] Sarkar demonstrated poly(β-myrcene) elastomers with M_n up to ∼93 kDa, and Anastasiou formulated green epoxy polymer poly(β-myrcene) epoxide.[53] Thus, poly(β-myrcene) may serve as a bioderived materials platform with controllable alkene concentration, stereo-

https://doi.org/10.1021/acsaem.3c02060
ACS Appl. Energy Mater. XXXX, XXX, XXX−XXX

Table 1. Characterization of the Various PME-TEMPO Species Quantifying the Stereochemical Ratios in the PβM Formulation, the Consumption of Alkenes to Epoxides in the PME-TEMPO, and the Successful Addition of TEMPO Groups along with Number Average Molecular Weight (M_n), Polymer Dispersity ($Đ$), and Glass Transition Temperature (T_g)

species	Myrcenea1,2 (%)	Myrcenea1,4 (%)	Myrcenea3,4 (%)	alkenes converted,[a] (%)	TEMPO incorporated,[a] (%)	M_n[a] (kDa)	M_n[b] (kDa)	$Đ$,[b]	T_g[c] (°C)
FR-50	4.5	67.7	27.9	32.9	50.8	5.2	5.4	1.10	62.0
FR-100	4.5	67.7	27.9	53.4	45.8	6.1	4.4	1.10	62.2
FR-150	4.5	67.7	27.9	58.6	44.4	6.5	3.8	1.29	59.8
FR-200	4.5	67.7	27.9	70.7	43.2	13.7	13.4	1.51	45.3
FRL-25	4.8	78.5	16.7	38.0	30.1	8.1	8.0	1.11	62.6
FRL-50	4.8	78.5	16.7	40.8	25.0	6.2	6.6	1.12	60.9
FRL-75	4.8	78.5	16.7	50.8	31.4	10.1	8.5	1.13	59.9
FRL-100	4.8	78.5	16.7	55.4	37.3	10.7	8.2	1.15	56.3
FRL-150	4.8	78.5	16.7	74.0	19.2	5.9	8.0	1.04	54.4
FRL-200	4.8	78.5	16.7	46.6	20.7	10.8	11.8	1.57	62.3
RAFT-25	6.4	75.5	19.6	46.6	20.0	21.5	23.8	1.16	58.0
RAFT-50	6.4	75.5	19.6	41.5	37.0	27.7	23.1	1.3	59.8
RAFT-100	6.4	75.5	19.6	62.0	15.8	25.9	28.4	1.19	58.5
RAFT-200	6.4	75.5	19.6	67.2	27.8	23.3	24.3	1.11	47.9

[a]As determined by proton (^{1}H) nuclear magnetic resonance (NMR). [b]As determined by size exclusion chromatography (SEC) against polystyrene (PS) standards. [c]Glass transition temperatures were determined by differential scanning calorimetry (DSC) on the second heating scan. These data were acquired after removal of the thermal history and scan rate was 10 °C min^{-1}. Note that no melting temperature was observed in any of the samples of these materials are completely amorphous.

chemistry, molecular weight, dispersity, and architecture with residual alkenes capable of post polymerization functionalization.

With these considerations in mind, we evaluated the suitability of poly(β-myrcene) in redox-active polymers. Using three different polymerization conditions, a series of alkene-containing, and later epoxide-laden, polymer precursors were synthesized. TEMPO moieties were installed onto the polymer chain at discrete functional group concentrations while maintaining sufficiently low T_g values, allowing for the quantification of the impact of the molecular structure on the electrochemical behavior. These bioderived aliphatic, nonconjugated, radical laden p-type materials are capable of ionic and electronic conduction while only requiring small amounts of external dopants. These energy storage materials achieved electronic conductivity levels of ~10^2 S cm^{-1} with minimal carbon black loading. Additional salt loading of these materials proved to improve electronic and ionic conductivity measures several orders of magnitude achieving measures of 10^{-3} S cm^{-1}. These hole-transporting radical polymers serve as green alternatives for cathode and electrolyte application and introduce the utility of bioderived materials as potential backbone alternatives for energy storage materials in organic sustainable batteries.

RESULTS AND DISCUSSION

An, aliphatic, nonconjugated radical homopolymer, poly(β-myrcene) (PβM), was synthesized from β-myrcene (Figure S1) using three synthetic methods: a free radical polymerization (FR, M_n ~4 kDa, $Đ$ ~1.62), a free radical polymerization with the inclusion of limonene as a mediating solvent (FRL, M_n ~5 kDa, $Đ$ ~2.34), and a reversible addition−fragmentation chain transfer polymerization (RAFT, M_n ~19 kDa, $Đ$ ~1.21) (Table S1). These polymers were subsequently epoxidized into poly(myrcene-epoxide) (PME), where the epoxide groups were later functionalized with 4-hydroxy-2,2,6,6-tetramethylpiperidin-1-oxyl (4-hydroxy-TEMPO) groups through base-catalyzed ring-opening reactions to yield organic radical-laden pendant groups as the bioderived energetic poly(myrcene-epoxide) TEMPO (PME-TEMPO), as shown in Figure 1.

The successful synthesis of the PβM polymer was confirmed using ^{1}H nuclear magnetic resonance (NMR) and Fourier transform infrared (FTIR) spectroscopy. The PβM displayed three characteristic resonances at 5.4, 5.13, and 4.78 ppm, which are associated with the 1,2, 1,4, and 3,4 myrcene linkages, respectively, and all three synthetic techniques yielded materials displaying these molecular architectures (Figures S2−S4).[51,54] The PβM was epoxidized using *meta*-chloroperbenzoic acid (*m*CPBA), previously shown to be successful in epoxidizing PβMs, yielding PME.[55] The successful epoxidation was confirmed by ^{1}H NMR spectroscopy, where the formation of the peak at approximately 2.75 ppm indicated epoxide formation, as did the reduction in the characteristic alkene peaks (Figure S5 and S6).[55,56] With the epoxides successfully attached to the backbone as the pendant groups of PME, subsequent ring-opening reactions using 1,8-diazabicyclo[5.4.0]undec-7-ene (DBU) were utilized to attach TEMPO radical groups to create the radical-containing macromolecule, PME-TEMPO. An emerging ^{1}H NMR resonance at 3.98 ppm was observed, and this region is characteristic of the C−H atoms on the six-membered rings of the nitroxide functionality of TEMPO. There is also a broad peak at 3.68 ppm indicating the presence of OH-groups resultant of the successful opening of the epoxides (Figures S7−S11). The successful epoxide ring-opening is also observed in the FTIR spectrum with a peak at 3439 cm^{-1} corresponding with the presence of pendant and backbone −OH groups on the PME-TEMPO materials, consistent with all three synthetic methods (Figure S12).

As expected, there is a slight increase in molecular weight observed by shifts to smaller retention times in the size exclusion chromatography (SEC) chromatograms with each synthetic step corresponding to larger pendant groups being attached (Figure 1c). The three synthetic methods resulted in a larger concentration (~70−80%) of 1,4 linkages compared to

https://doi.org/10.1021/acsaem.3c02060
ACS Appl. Energy Mater. XXXX, XXX, XXX−XXX

3,4 and 1,2 with the FRL and RAFT methods producing the highest percentages of 1,4 linkages which is consistent with previous findings reports (Table 1).[48,51,54] Subspecies were created of each synthetic method, FR, FRL, and RAFT, according to the amount of alkenes capable of epoxidation due to the amount of *m*CPBA used (FR-50 meaning enough *m*CPBA is present to epoxidize 50% of alkenes). With increasing *m*CPBA present, an increasing number of alkene groups were converted to epoxide groups achieving up to 74% of alkenes converted (Table 1). The ring-opening reactions allowed for the attachment of ~50% of TEMPO groups onto the opened epoxides while showing high control over all the species ($1.1 < Đ < 1.6$) (Table 1).

All products had $T_g < -40$ °C (Table 1). These low T_g values are advantageous regarding potential additional processing as they are well below the thermal degradation temperature of the TEMPO moieties.

The TEMPO radical loading in the polymers is a crucial factor to the performance of these energy storage materials, as they are the only electrochemically active moieties in these polymers. The redox activity of the TEMPO radical was confirmed using cyclic voltammetry with a peak-to-peak width of 0.12 V and an oxidation peak occurring at approximately +0.8 V, consistent with other macromolecules containing TEMPO radicals, in representative cyclic voltammograms of FR-200, FRL-200, and RAFT-200 (Figure 2).[57] This behavior

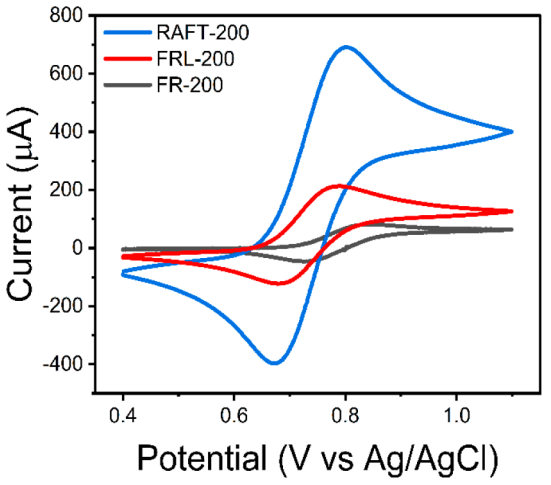

Figure 2. Representative cyclic voltammograms (CVs) of FR, FRL, and RAFT PME-TEMPO species showing the oxidation and reduction reactions of the TEMPO radical. An electrolyte solution of 0.1 M tetrabutylammonium hexafluorophosphate ($TBAPF_6$) in acetonitrile was used with scan rates of 50 mV $s^{-1}$and a polymer concentration of 10 mg mL^{-1}.

is consistent with the PME-TEMPO species on the other end of the spectra as well (Figure S13). The presence of radicals on the TEMPO pendant groups was quantified using electron paramagnetic resonance (EPR) spectroscopy, which showed peaks in the range of 3480 and 3520 G across all PME-TEMPO species (Figure S15).

This behavior is consistent with other aliphatic, non-conjugated redox-active materials containing TEMPO radicals.[23,58] Radical content measurements were calculated from doubly integrating the EPR signal intensities and comparing with those of a TEMPO−OH standard as 100% radical content (Table S2). The FR and FRL PME-TEMPO species generally had higher radical density over the RAFT formulations with all but two formulations having over 50% radical content and only one of the RAFT formulations having over 50% radical content (Table S2). Transporting charge between radical sites is heavily related to the radical density, so to narrow the scope of material testing, the four subspecies with the highest radical content (FR-100, FR-150, FRL-75, and FRL-100) were selected for conductivity testing (Table S2).

The PME-TEMPO species had relatively low electrical conductivities (σ_e) of ~3×10^{-8} S cm^{-1}, as shown in the current−voltage plot of Figure S16. This is not unusual for nonconjugated polymers with low radical functionalization as they are considered insulators; however, to have any significant performance, the addition of a conducting filler to achieve higher conductance values is needed. Carbon is commonly added to improve conductivity capabilities, particularly in composite electrodes. Thus, the materials were combined with 5% and 15% carbon black (by weight) to increase the conductivity values to a suitable level for cathode applications (Figure 3).[37]

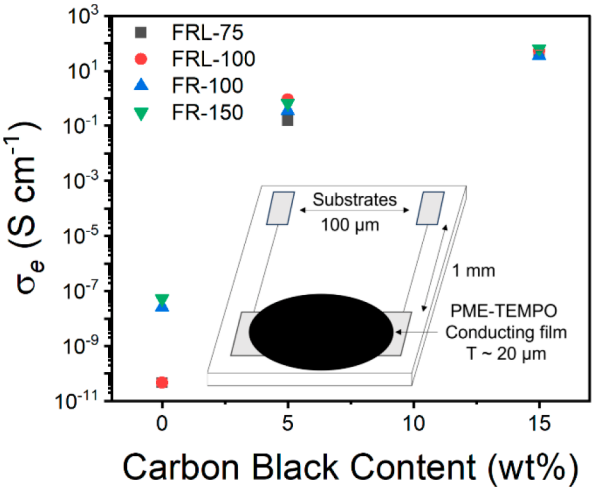

Figure 3. Electrical conductivity of the PME-TEMPO composites as a function of carbon black loading. Note that the data points shown are the averages of three trials and the standard deviations of the averages are smaller than the data points. The device schematic used for the study is inset.

There was a marked increase in conductivity values corresponding to the increase in carbon black loading reaching values >60 S cm^{-1} at 15% loading, achieving electrical conductivity values on par with other cathode material conductivities (Table S3).[59] Other studies report significantly larger carbon black loadings such as 60 wt % and up to an 8:1 weight ratio of carbon black to polymer weight to get comparable conductivities.[37,60] The significant increase in conductivity indicates that with minimal carbon black loading (i.e., 5 wt % relative to the polymer), the carbon black additive is the driving force in the conductivity levels.

Adding ionic salts to composite polymer electrodes is an effective strategy to create mixed ionic and electronic conducting energy storage materials.[61] To quantify the effect of salt-mixing on the conductivity of the PME-TEMPO materials, two lithium-based salts were loaded into the polymer. The first was lithium hexafluorophosphate ($LiPF_6$) as it is a common salt used in electrolyte solutions for lithium-ion batteries.[62] The second selected salt was lithium chloride

https://doi.org/10.1021/acsaem.3c02060
ACS Appl. Energy Mater. XXXX, XXX, XXX−XXX

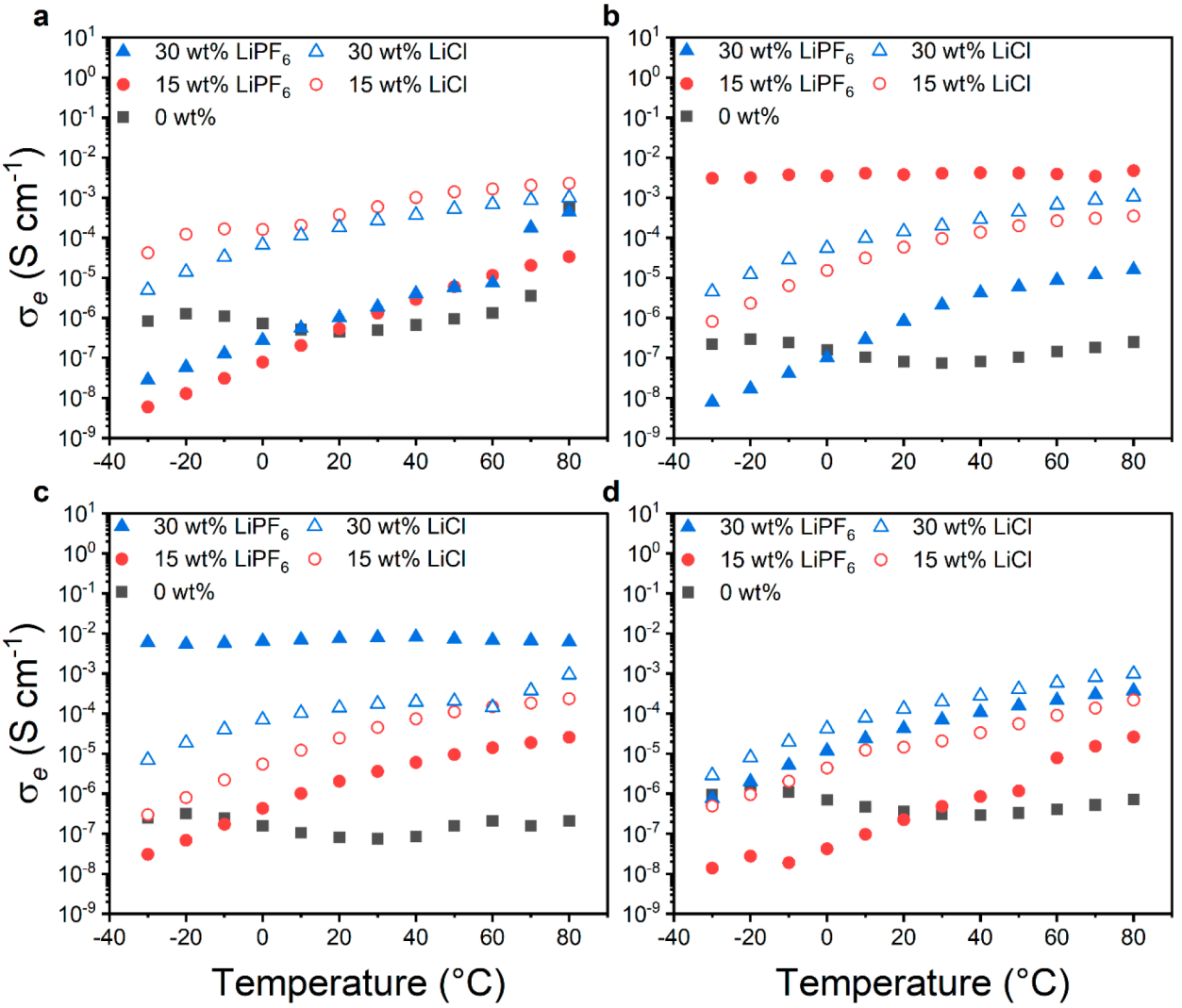

Figure 4. Electrical conductivity of (a) FRL-75, (b) FRL-100, (c) FR-100, and (d) FR-150 PME-TEMPO materials with increasing Li salt loadings at a frequency of 10^6 Hz as a function of temperature.

(LiCl) as $LiPF_6$ has shown to be relatively chemically instable and unsafe, particularly when flammable, low boiling point solvents are used and LiCl has shown to be more biotolerable.[62−64] Respective salt amounts (15 and 30 wt %) of total sample mass were dissolved in the PME-TEMPO materials and methanol-chloroform solvent mix and were subsequently dried under vacuum. Frequency sweeps were conducted on the raw and salt-loaded materials at temperatures ranging from $-30\ °C \leq T \leq 80\ °C$ (Figures S19−S20). There was an expected rise of conductivity values with the increase in frequency across the board in all formulations along with the increase in temperature. To investigate electron transport as a function of salt loading, upper frequency conductivities (10^6 Hz) were measured on a temperature sweep. The incorporation of Li ions proved to increase the electronic conductivity of the PME-TEMPO materials increasing up to $\sim 10^{-5}$ S cm^{-1} in the $LiPF_6$ loaded formulations from the pristine PME-TEMPO materials (Figure 4b,c). The higher salt loading ($LiPF_6$ and LiCl) generally led to higher electronic conductivity levels likely due to the enhanced mixed conduction of the Li-ion loading providing greater electron transport properties in the polymers. This could be due to multiple factors increasing the charge transport such as ionic-electronic coupling, and electronic and ionic transport. This was apart from the FRL-100 material as the 15 wt % had a higher conductivity than the 30 wt % (Figure 4b). Despite there being a higher ion concentration indicating there should be a uniform increase in electronic conductivity, the higher salt loading could affect segmental motions within the PME-TEMPO materials which would affect the electron and ion transport of the materials.[65] In general, the LiCl loaded polymers had higher conductivities than the $LiPF_6$ formulations. This is except for FRL-100 formulation at 15 wt %, and FR-100 at 30 wt % which ranged from three-to-one orders magnitude of electrical conductivity higher than the mirrored LiCl formulations (Figure 4b,c). This is likely due to LiCl being more soluble in the PME-TEMPO materials than the $LiPF_6$ leading to greater electron−ion interactions and facilitating higher degrees of electron transport. The 30 wt % LiCl formulations all had higher conductivity levels in all PME-TEMPO materials with exception of the FRL-75 formulations as the 15 wt % LiCl was roughly half an order of magnitude higher than FRL-75 30 wt % LiCl across the entire temperature sweep again likely due to the impaired PME-TEMPO segmental motion from higher salt loading (Figure 4a). All formulations with both lithium salts were able to achieve

https://doi.org/10.1021/acsaem.3c02060
ACS Appl. Energy Mater. XXXX, XXX, XXX−XXX

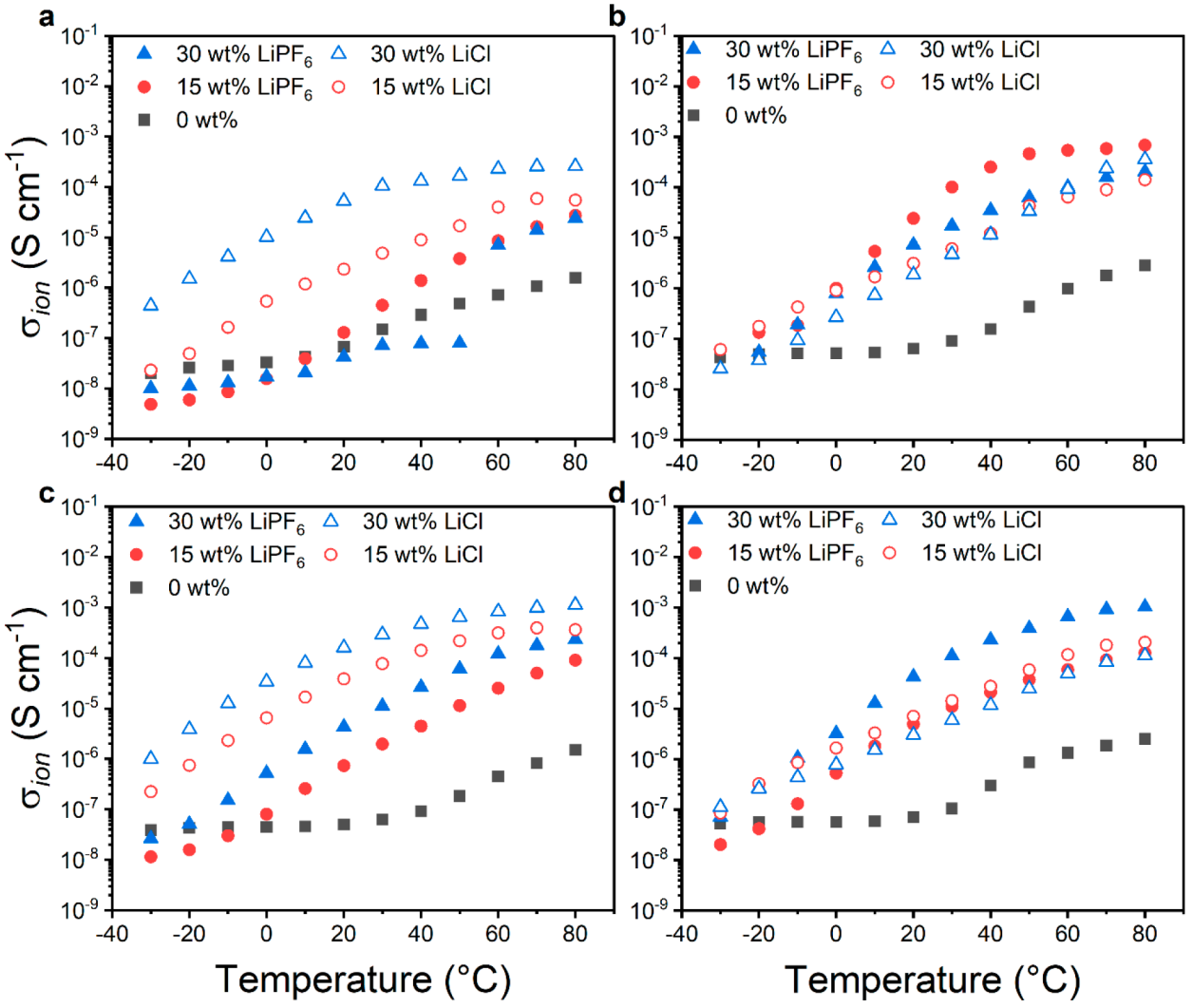

Figure 5. Ionic conductivity of (a) FRL-75, (b) FRL-100, (c) FR-100, and (d) FR-150 PME-TEMPO materials with increasing Li salt loadings at a frequency of 10^4 Hz as a function of temperature.

$\sim 10^{-4}$ S cm^{-1} while FRL-75 using 15 wt % LiCl, FRL-100 using 15 wt % $LiPF_6$, and FR-100 using 30 wt % $LiPF_6$ were able to reach conductivity levels of 10^{-3} S cm^{-1} (Figure 4). With few exceptions, the doping of Li ions provided a straightforward manner of mixed conduction allowing as much as an increase of 4 orders of magnitude in electrical conductivity performance opposed to the pristine PME-TEMPO materials.

For the PME-TEMPO materials to replace traditional solvent-based electrolyte mediums, they must be capable of ion transport. To isolate ionic conductivity in the Li salt doped PME-TEMPO materials, a similar evaluation was conducted using poly(ethylene oxide) insulating blocking layers between the two gold electrodes and the radical polymer and evaluating ionic conductivity levels at 10^4 Hz (Figures S22–S23). The pristine PME-TEMPO materials had baseline conductivity values of $\sim 10^{-6}$ S cm^{-1}, too low for significant electrolyte application (Figure 5). In similar fashion with the electrical conductivity values, the overall ionic conductivity increased with the presence of Li salt. Ionic conductivity levels increased at least 4 orders of magnitude across all PME-TEMPO formulations due to the increase of ion concentration (Figure 5). This highlighted that the incorporation of the increased ion transport capabilities of the polymer. The LiCl formulations produced higher ionic conductivity levels than the $LiPF_6$ formulations in all but two formulations: FRL-100 15 wt % and FR-150 30 wt % both reported higher ionic conductivities with $LiPF_6$. This is likely due to an increased ion mobility in those specific formulations and salt concentrations with $LiPF_6$ leading to a higher degree of ion transport. Increasing the salt concentration in the PME-TEMPO materials generally lead to an increase in ionic conductivity with three exceptions, the 15 wt % $LiPF_6$ FRL-100 formulation had higher conductivity measurements ($\sim 2.0 \times 10^{-4}$ S cm^{-1}) than the 30 wt % $LiPF_6$ formulation ($\sim 7.0 \times 10^{-4}$ S cm^{-1}) at 80 °C along with the 15 wt % FR-150 LiCl formulation as well having a conductivity value of $\sim 2.0 \times 10^{-4}$ S cm^{-1} and the 30 wt % LiCl formulation had a conductivity value of $\sim 1.0 \times 10^{-4}$ S cm^{-1} (Figure 5b and d). This again is likely resultant of the increased Li ion concentration leading to impaired segment mobility of the polymer which impairs the ability of ion transport effecting ionic conductivity. Despite the few exceptions, this behavior still shows that doping the PME-TEMPO materials with Li ions provides a straightforward method if increasing the ionic conductivity. Both Li salts produced formulations with ionic of 10^{-3} S cm^{-1} 30 wt % salt incorporation at 80 °C, 6 orders of

https://doi.org/10.1021/acsaem.3c02060
ACS Appl. Energy Mater. XXXX, XXX, XXX−XXX

magnitude above the pristine polymers (Figure 5). Once doped with the Li salts, the PME-TEMPO materials were able to achieve conductivity measurements on par with other electrolyte solutions for ion transport showing potential for a polymer electrolyte in a battery application.[66,67]

CONCLUSIONS

The bioderived PME-TEMPO materials synthesized from β-myrcene serve as aliphatic, nonconjugated p-type materials capable of facilitating redox reactions between neighboring radical sites on TEMPO pendant groups. While in their pristine (i.e., not doped) states, these materials do not provide sufficient conductance values to serve as a cathode material or electrolyte medium, when combined with external loadings or carbonaceous material and Li-salt, their performances dramatically increase. When blended with as little as 5% carbon black, the conductivity increased up to 10 orders of magnitude where similar loadings have reported conductivities of $\sim 10^{-7}$ S cm^{-1}.[68] When blending with either lithium hexafluorophosphate and lithium chloride, these materials serve as mixed ionic-electronic conductors with electronic conductivity values increasing up to 3 orders of magnitude at 80 °C and higher frequencies (10^6 Hz) and ionic conductivity values increasing 2 orders of magnitude at 80 °C and 10^4 Hz. These elevated metrics with the combination of external materials show potential application for energy storage. These materials provide an attractive, bioderived alternative for cathode and polymer electrolyte application for sustainable organic batteries.

ASSOCIATED CONTENT

Supporting Information

The Supporting Information is available free of charge at https://pubs.acs.org/doi/10.1021/acsaem.3c02060.

Methods and materials, as well as spectroscopic characterizations, including ^{1}H NMR, FT-IR, and dielectric spectroscopy, SEC, DSC, FT-IR, EPR, cyclic voltammograms, current−voltage curves and calculations, and preparation and characterization of blocking electrodes (PDF)

AUTHOR INFORMATION

Corresponding Authors

Andrew C. Weems − *Department of Mechanical Engineering and Biomedical Engineering, Translational Biomedical Sciences, Molecular and Chemical Biology, Ohio Musculoskeletal and Neurological Institute, Center for Advanced Materials Processing, Ohio University, Athens, Ohio 45701, United States;* orcid.org/0000-0001-6592-3015; Email: weemsac@ohio.edu

Bryan W. Boudouris − *Charles D. Davidson School of Chemical Engineering, Purdue University, West Lafayette, Indiana 47907, United States; Department of Chemistry, Purdue University, West Lafayette, Indiana 47907, United States;* orcid.org/0000-0003-0428-631X; Email: boudouris@purdue.edu

Authors

Scott L. Brooks − *Department of Mechanical Engineering, Ohio University, Athens, Ohio 45701, United States*

Zihao Liang − *Charles D. Davidson School of Chemical Engineering, Purdue University, West Lafayette, Indiana 47907, United States*

Hyunki Yeo − *Charles D. Davidson School of Chemical Engineering, Purdue University, West Lafayette, Indiana 47907, United States*

Complete contact information is available at: https://pubs.acs.org/10.1021/acsaem.3c02060

Notes

The authors declare no competing financial interest.

ACKNOWLEDGMENTS

The authors would like to thank the Department of Energy for Weems's startup funds. Additionally, we are grateful to the Ohio NASA Space Consortium and the Department of Education's GAANN fellowship for funding S Brooks. The work at Purdue University was supported by the US Department of Energy, Office of Science, Basic Energy Sciences, under award DE-SC0021967 (Program Manager: Dr. Craig Henderson), and we thank the Department of Energy for this generous support.

REFERENCES

(1) Tomlinson, E. P.; Hay, M. E.; Boudouris, B. W. Radical Polymers and Their Application to Organic Electronic Devices. *Macromolecules* **2014**, *47* (18), 6145−6158.

(2) Friebe, C.; Lex-Balducci, A.; Schubert, U. S. Sustainable Energy Storage: Recent Trends and Developments toward Fully Organic Batteries. *ChemSusChem* **2019**, *12* (18), 4093−4115.

(3) Kim, J.; Kim, J. H.; Ariga, K. Redox-Active Polymers for Energy Storage Nanoarchitectonics. *Joule* **2017**, *1* (4), 739−768.

(4) Holliday, S.; Donaghey, J. E.; McCulloch, I. Advances in charge carrier mobilities of semiconducting polymers used in organic transistors. *Chem. Mater.* **2014**, *26* (1), 647−663.

(5) Chi, T.; Akkiraju, S.; Liang, Z.; Tan, Y.; Kim, H. J.; Zhao, X.; Savoie, B. M.; Boudouris, B. W. Design of an n-type low glass transition temperature radical polymer. *Polym. Chem.* **2021**, *12* (10), 1448−1457.

(6) Cheng, F.; Bonder, E. M.; Jäkle, F. Electron-Deficient Triarylborane Block Copolymers: Synthesis by Controlled Free Radical Polymerization and Application in the Detection of Fluoride Ions. *J. Am. Chem. Soc.* **2013**, *135* (46), 17286−17289.

(7) Joo, Y.; Agarkar, V.; Sung, S. H.; Savoie, B. M.; Boudouris, B. W. A nonconjugated radical polymer glass with high electrical conductivity. *Science* **2018**, *359* (6382), 1391−1395.

(8) Rostro, L.; Baradwaj, A. G.; Boudouris, B. W. Controlled Radical Polymerization and Quantification of Solid State Electrical Conductivities of Macromolecules Bearing Pendant Stable Radical Groups. *ACS Appl. Mater. Interfaces* **2013**, *5* (20), 9896−9901.

(9) Merckle, D.; King, O.; Weems, A. C. Ring-Opening Copolymerization of Four-Dimensional Printable Polyesters Using Supramolecular Thiourea/Organocatalysis. *ACS Sustainable Chem. Eng.* **2023**, *11* (6), 2219−2228.

(10) Suga, T.; Nishide, H. Redox-Active Radical Polymers for a Totally Organic Rechargeable Battery. In *Polymers for Energy Storage and Delivery: Polyelectrolytes for Batteries and Fuel Cells*, ACS Symposium Series, Vol. *1096*; American Chemical Society: Washington, D.C., 2012; pp 45−53 DOI: 10.1021/bk-2012-1096.ch003.

(11) Nikiforov, M. P.; Lai, B.; Chen, W.; Chen, S.; Schaller, R. D.; Strzalka, J.; Maser, J.; Darling, S. B. Detection and role of trace impurities in high-performance organic solar cells. *Energy Environ. Sci.* **2013**, *6* (5), 1513−1520.

(12) Krebs, F. C.; Nyberg, R. B.; Jørgensen, M. Influence of Residual Catalyst on the Properties of Conjugated Polyphenylenevinylene

Materials: Palladium Nanoparticles and Poor Electrical Performance. *Chem. Mater.* **2004**, *16* (7), 1313−1318.
(13) Huo, M.; Yuan, J.; Tao, L.; Wei, Y. Redox-responsive polymers for drug delivery: from molecular design to applications. *Polym. Chem.* **2014**, *5* (5), 1519−1528.
(14) Sui, X.; Feng, X.; Hempenius, M. A.; Vancso, G. J. Redox active gels: synthesis, structures and applications. *J. Mater. Chem. B* **2013**, *1* (12), 1658−1672.
(15) Janoschka, T.; Friebe, C.; Hager, M. D.; Martin, N.; Schubert, U. S. An Approach Toward Replacing Vanadium: A Single Organic Molecule for the Anode and Cathode of an Aqueous Redox-Flow Battery. *ChemistryOpen* **2017**, *6* (2), 216−220.
(16) Oyaizu, K.; Nishide, H. Radical Polymers for Organic Electronic Devices: A Radical Departure from Conjugated Polymers? *Adv. Mater.* **2009**, *21* (22), 2339−2344.
(17) Wingate, A. J.; Boudouris, B. W. Recent advances in the syntheses of radical-containing macromolecules. *J. Polym. Sci., Part A: Polym. Chem.* **2016**, *54* (13), 1875−1894.
(18) Hung, M.-K.; Wang, Y.-H.; Lin, C.-H.; Lin, H.-C.; Lee, J.-T. Synthesis and electrochemical behaviour of nitroxide polymer brush thin-film electrodes for organic radical batteries. *J. Mater. Chem.* **2012**, *22* (4), 1570−1577.
(19) Janoschka, T.; Teichler, A.; Krieg, A.; Hager, M. D.; Schubert, U. S. Polymerization of free secondary amine bearing monomers by RAFT polymerization and other controlled radical techniques. *J. Polym. Sci., Part A: Polym. Chem.* **2012**, *50* (7), 1394−1407.
(20) Shipp, D. A. Living radical polymerization: Controlling molecular size and chemical functionality in vinyl polymers. *Journal of Macromolecular Science, Part C: Polymer Reviews* **2005**, *45* (2), 171−194.
(21) Gao, H.; Matyjaszewski, K. Synthesis of functional polymers with controlled architecture by CRP of monomers in the presence of cross-linkers: From stars to gels. *Prog. Polym. Sci.* **2009**, *34* (4), 317−350.
(22) Oyaizu, K.; Kawamoto, T.; Suga, T.; Nishide, H. Synthesis and Charge Transport Properties of Redox-Active Nitroxide Polyethers with Large Site Density. *Macromolecules* **2010**, *43* (24), 10382−10389.
(23) Rostro, L.; Wong, S. H.; Boudouris, B. W. Solid State Electrical Conductivity of Radical Polymers as a Function of Pendant Group Oxidation State. *Macromolecules* **2014**, *47* (11), 3713−3719.
(24) Ramesh, S.; Arof, A. K. Electrical conductivity studies of polyvinyl chloride-based electrolytes with double salt system. *Solid State Ionics* **2000**, *136* (1-2), 1197−1200.
(25) Kola, S.; Sinha, J.; Katz, H. E. Organic transistors in the new decade: Toward n-channel, printed, and stabilized devices. *J. Polym. Sci., Part B: Polym. Phys.* **2012**, *50* (15), 1090−1120.
(26) Kamtekar, K. T.; Monkman, A. P.; Bryce, M. R. Recent advances in white organic light-emitting materials and devices (WOLEDs). *Adv. Mater.* **2010**, *22* (5), 572−582.
(27) Nakahara, K.; Oyaizu, K.; Nishide, H. Organic radical battery approaching practical use. *Chemistry letters* **2011**, *40* (3), 222−227.
(28) Suga, T.; Sakata, M.; Aoki, K.; Nishide, H. Synthesis of Pendant Radical- and Ion-Containing Block Copolymers via Ring-Opening Metathesis Polymerization for Organic Resistive Memory. *ACS Macro Lett.* **2014**, *3* (8), 703−707.
(29) Yonekuta, Y.; Susuki, K.; Oyaizu, K.; Honda, K.; Nishide, H. Battery-Inspired, Nonvolatile, and Rewritable Memory Architecture: a Radical Polymer-Based Organic Device. *J. Am. Chem. Soc.* **2007**, *129* (46), 14128−14129.
(30) Nishide, H.; Koshika, K.; Oyaizu, K. Environmentally benign batteries based on organic radical polymers. *Pure and applied chemistry* **2009**, *81* (11), 1961−1970.
(31) Oyaizu, K.; Sukegawa, T.; Nishide, H. Dual dopable poly (phenylacetylene) with nitronyl nitroxide pendants for reversible ambipolar charging and discharging. *Chem. Lett.* **2011**, *40* (2), 184−185.
(32) Suga, T.; Pu, Y.-J.; Oyaizu, K.; Nishide, H. Electron-transfer kinetics of nitroxide radicals as an electrode-active material. *Bull. Chem. Soc. Jpn.* **2004**, *77* (12), 2203−2204.
(33) Nishide, H.; Suga, T. Organic Radical Battery. *Electrochemical Society Interface* **2005**, *14* (4), 32.
(34) Oyaizu, K.; Suga, T.; Yoshimura, K.; Nishide, H. Synthesis and Characterization of Radical-Bearing Polyethers as an Electrode-Active Material for Organic Secondary Batteries. *Macromolecules* **2008**, *41* (18), 6646−6652.
(35) Liang, Z.; Hsu, S.-N.; Tan, Y.; Tahir, H.; Kim, H. J.; Liu, K.; Stoehr, J. F.; Zeller, M.; Dou, L.; Savoie, B. M.; Boudouris, B. W. Significant charge transport effects due to subtle molecular changes in nitroxide radical single crystals. *Cell Reports Physical Science* **2023**, *4* (5), No. 101409.
(36) Liang, Z.; Tan, Y.; Hsu, S.-N.; Stoehr, J. F.; Tahir, H.; Woeppel, A. B.; Debnath, S.; Zeller, M.; Dou, L.; Savoie, B. M.; Boudouris, B. W. Charge transport and antiferromagnetic ordering in nitroxide radical crystals. *Molecular Systems Design & Engineering* **2023**, *8* (4), 464−472.
(37) Nguyen, T. P.; Easley, A. D.; Kang, N.; Khan, S.; Lim, S.-M.; Rezenom, Y. H.; Wang, S.; Tran, D. K.; Fan, J.; Letteri, R. A.; He, X.; Su, L.; Yu, C.-H.; Lutkenhaus, J. L.; Wooley, K. L. Polypeptide organic radical batteries. *Nature* **2021**, *593* (7857), 61−66.
(38) Robert, C.; de Montigny, F.; Thomas, C. M. Tandem synthesis of alternating polyesters from renewable resources. *Nat. Commun.* **2011**, *2* (1), 586.
(39) Chamas, A.; Moon, H.; Zheng, J.; Qiu, Y.; Tabassum, T.; Jang, J. H.; Abu-Omar, M.; Scott, S. L.; Suh, S. Degradation Rates of Plastics in the Environment. *ACS Sustainable Chem. Eng.* **2020**, *8* (9), 3494−3511.
(40) Thomsett, M. R.; Moore, J. C.; Buchard, A.; Stockman, R. A.; Howdle, S. M. New renewably-sourced polyesters from limonene-derived monomers. *Green Chem.* **2019**, *21* (1), 149−156.
(41) Della Monica, F.; Kleij, A. W. From terpenes to sustainable and functional polymers. *Polym. Chem.* **2020**, *11* (32), 5109−5127.
(42) O'Brien, D. M.; Atkinson, R. L.; Cavanagh, R.; Pacheco, A. A.C.; Larder, R.; Kortsen, K.; Krumins, E.; Haddleton, A. J.; Alexander, C.; Stockman, R. A.; Howdle, S. M.; Taresco, V. A 'greener'one-pot synthesis of monoterpene-functionalised lactide oligomers. *Eur. Polym. J.* **2020**, *125*, No. 109516.
(43) Singh, A.; Kamal, M. Synthesis and characterization of polylimonene: Polymer of an optically active terpene. *J. Appl. Polym. Sci.* **2012**, *125* (2), 1456−1459.
(44) Guggenbiller, G.; Brooks, S.; King, O.; Constant, E.; Merckle, D.; Weems, A. C. 3D Printing of Green and Renewable Polymeric Materials: Toward Greener Additive Manufacturing. *ACS Applied Polymer Materials* **2023**, *5*, 3201.
(45) Claudino, M.; Mathevet, J.-M.; Jonsson, M.; Johansson, M. Bringing d-limonene to the scene of bio-based thermoset coatings via free-radical thiol−ene chemistry: macromonomer synthesis, UV-curing and thermo-mechanical characterization. *Polym. Chem.* **2014**, *5* (9), 3245−3260.
(46) Weems, A. C.; Delle Chiaie, K. R.; Worch, J. C.; Stubbs, C. J.; Dove, A. P. Terpene- and terpenoid-based polymeric resins for stereolithography 3D printing. *Polym. Chem.* **2019**, *10* (44), 5959−5966.
(47) Sharma, S.; Srivastava, A. K. Radical co-polymerization of limonene with N-vinyl pyrrolidone: synthesis and characterization. *Des. Monomers Polym.* **2006**, *9* (5), 503−516.
(48) Bauer, N.; Brunke, J.; Kali, G. Controlled Radical Polymerization of Myrcene in Bulk: Mapping the Effect of Conditions on the System. *ACS Sustainable Chem. Eng.* **2017**, *5* (11), 10084−10092.
(49) Hilschmann, J.; Kali, G. Bio-based polymyrcene with highly ordered structure via solvent free controlled radical polymerization. *Eur. Polym. J.* **2015**, *73*, 363−373.
(50) Naddeo, M.; Buonerba, A.; Luciano, E.; Grassi, A.; Proto, A.; Capacchione, C. Stereoselective polymerization of biosourced terpenes β-myrcene and β-ocimene and their copolymerization with styrene promoted by titanium catalysts. *Polymer* **2017**, *131*, 151−159.

https://doi.org/10.1021/acsaem.3c02060
ACS Appl. Energy Mater. XXXX, XXX, XXX−XXX

(51) Constant, E.; King, O.; Weems, A. C. Bioderived 4D Printable Terpene Photopolymers from Limonene and β-Myrcene. *Biomacromolecules* **2022**, *23* (6), 2342−2352.
(52) Weems, A. C.; Delle Chiaie, K. R.; Yee, R.; Dove, A. P. Selective Reactivity of Myrcene for Vat Photopolymerization 3D Printing and Post-Fabrication Surface Modification. *Biomacromolecules* **2020**, *21* (1), 163−170.
(53) Anastasiou, D. E. Investigating the Epoxidation of Poly-β-myrcene: Optimization, Kinetics, and Thermodynamics. *Journal of Polymers and the Environment* **2023**, *31*, 4044.
(54) Zhang, J.; Aydogan, C.; Patias, G.; Smith, T.; Al-Shok, L.; Liu, H.; Eissa, A. M.; Haddleton, D. M. Polymerization of Myrcene in Both Conventional and Renewable Solvents: Postpolymerization Modification via Regioselective Photoinduced Thiol−Ene Chemistry for Use as Carbon Renewable Dispersants. *ACS Sustainable Chem. Eng.* **2022**, *10* (29), 9654−9664.
(55) Matic, A.; Hess, A.; Schanzenbach, D.; Schlaad, H. Epoxidized 1,4-polymyrcene. *Polym. Chem.* **2020**, *11* (7), 1364−1368.
(56) Tibbetts, J. D.; Cunningham, W. B.; Vezzoli, M.; Plucinski, P.; Bull, S. D. Sustainable catalytic epoxidation of biorenewable terpene feedstocks using H2O2 as an oxidant in flow microreactors. *Green Chem.* **2021**, *23* (15), 5449−5455.
(57) Cheng, Y.; Hall, D.; Boualavong, J.; Hickey, R.; Lvov, S.; Gorski, C. Influence of Hydrotropes on the Solubilities and Diffusivities of Redox-Active Organic Compounds for Aqueous Flow Batteries. *ACS Omega* **2021**, *6*, 30800−30810.
(58) Zhang, J.; Shen, H.; Song, W.; Wang, G. Synthesis and Characterization of Novel Copolymers with Different Topological Structures and TEMPO Radical Distributions. *Macromolecules* **2017**, *50* (7), 2683−2695.
(59) El-Tantawy, F.; Kamada, K.; Ohnabe, H. In situ network structure, electrical and thermal properties of conductive epoxy resin−carbon black composites for electrical heater applications. *Mater. Lett.* **2002**, *56* (1), 112−126.
(60) Wu, X.; Liu, M.; Yao, S.; Li, S.; Pang, S.; Shen, X.; Li, T.; Qin, S. Boosting the electrochemical performance of lithium-sulfur batteries by using a carbon black/LiMn2O4-modified separator. *J. Alloys Compd.* **2020**, *835*, No. 155251.
(61) Li, X.; Liu, Z.; Zhou, Z.; Gao, H.; Liang, G.; Rauber, D.; Kay, C. W. M.; Zhang, P. Effects of Cationic Species in Salts on the Electrical Conductivity of Doped PEDOT:PSS Films. *ACS Applied Polymer Materials* **2021**, *3* (1), 98−103.
(62) Wang, Q.; Jiang, L.; Yu, Y.; Sun, J. Progress of enhancing the safety of lithium ion battery from the electrolyte aspect. *Nano Energy* **2019**, *55*, 93−114.
(63) Nikiforidis, G.; Raghibi, M.; Sayegh, A.; Anouti, M. Low-Concentrated Lithium Hexafluorophosphate Ternary-based Electrolyte for a Reliable and Safe NMC/Graphite Lithium-Ion Battery. *J. Phys. Chem. Lett.* **2021**, *12* (7), 1911−1917.
(64) Zhang, J.; He, L.; Yang, Z.; Li, L.; Cai, W. Lithium chloride promotes proliferation of neural stem cells in vitro, possibly by triggering the Wnt signaling pathway. *Animal Cells and Systems* **2019**, *23* (1), 32−41.
(65) Zhao, Y.; Tao, R.; Fujinami, T. Enhancement of ionic conductivity of PEO-LiTFSI electrolyte upon incorporation of plasticizing lithium borate. *Electrochim. Acta* **2006**, *51* (28), 6451−6455.
(66) Ding, Y.; Zhang, P.; Long, Z.; Jiang, Y.; Xu, F.; Di, W. The ionic conductivity and mechanical property of electrospun P(VdF-HFP)/PMMA membranes for lithium ion batteries. *J. Membr. Sci.* **2009**, *329* (1), 56−59.
(67) Fan, F. Y.; Pan, M. S.; Lau, K. C.; Assary, R. S.; Woodford, W. H.; Curtiss, L. A.; Carter, W. C.; Chiang, Y.-M. Solvent effects on polysulfide redox kinetics and ionic conductivity in lithium-sulfur batteries. *J. Electrochem. Soc.* **2016**, *163* (14), A3111.
(68) Burmistrov, I.; Gorshkov, N.; Ilinykh, I.; Muratov, D.; Kolesnikov, E.; Anshin, S.; Mazov, I.; Issi, J. P.; Kusnezov, D. Improvement of carbon black based polymer composite electrical conductivity with additions of MWCNT. *Compos. Sci. Technol.* **2016**, *129*, 79−85.

https://doi.org/10.1021/acsaem.3c02060
ACS Appl. Energy Mater. XXXX, XXX, XXX−XXX